Anharmonic Decay of Vibrational States in Helical Peptides, Coils, and One-Dimensional Glasses†

David M. Leitner

Department of Chemistry and Chemical Physics Program, University of Nevada, Reno, Nevada 89557

Received: March 4, 2002; In Final Form: May 31, 2002

Rates of vibrational energy transfer in the five largest α helices and two largest coil segments of myoglobin are calculated and compared with energy transfer in one-dimensional glasses. In all three cases, vibrational energy transfer occurs by anharmonic coupling of spatially overlapping localized normal modes in resonance. The frequencies of pairs of localized vibrational modes close in space are usually separated by a few hundred cm^{-1}. As a result, there is little direct energy transfer to low-frequency modes by low-order anharmonic coupling, and rates of vibrational energy transfer from most higher-frequency modes are nearly temperature-independent, consistent with experimental observations. Variation of the anharmonic decay rate with mode frequency in helices and coils is similar, the trends of which are captured by an appropriately parametrized one-dimensional glass.

1. Introduction

Describing chemical events in molecules and clusters ultimately requires a picture of the flow of energy on the picosecond time scale. Recent theoretical and experimental work has unraveled how energy flows quantum mechanically in small molecules,[1,2] and progress continues on connecting quantum energy flow in molecules to the kinetics of conformational change.[3,4] Rates of conformational isomerization of rather small molecules are often influenced by rates of intramolecular energy flow, as illustrated by the well-studied examples of cyclohexane ring inversion[4,5] and *trans*-stilbene photoisomerization.[3,6] Energy flow rates influence chemical reaction rates when energy transfer in to and out of transition states is slower than the vibrational frequency of crossing the barrier when the molecule goes through an activated complex. In many small molecules at barrier energies the former rate is of order 1 ps^{-1} or less while the latter is of order 10 ps^{-1}.[3,4] What is the rate of vibrational energy transfer in a large molecule, such as a protein? Unlike small molecules such as cyclohexane, a protein has a large density of low-frequency modes into which energy can flow. Any vibrational mode is directly coupled anharmonically to a very large number of these bath modes, which could in principle dramatically increase the energy transfer rate above 1 ps^{-1}. Recent spectroscopic studies[7,8,9] of the amide I band of a variety of globular peptides and proteins, however, suggest that energy transfer rates in proteins may not be very different from those in small molecules. Amide I band spectroscopy, which provides information about vibrational energy transfer from modes in the range 1600−1700 cm^{-1}, reveals typical values of the energy transfer rate that are of order 1 ps^{-1}, not unlike intramolecular energy flow rates in smaller molecules.[7,8] Moreover, the energy transfer rate from the amide I band of myoglobin appears to vary little with temperature from about 10 to 300 K.[7] These observations suggest that there is little direct energy transfer from the amide I vibration to the bath of low-frequency protein modes. Spectroscopic studies of CO−myoglobin by Fayer, Dlott, and co-workers[10,11] similarly reveal that the decay rate of vibrational energy from the ligand to the protein is nearly independent of temperature, again from about 10 to 300 K. Another feature that may influence energy flow in large molecules is structure. While anharmonicity plays a pivotal role in a protein's vibrational dynamics and energy transfer,[12,13] it has also been suggested that certain structural features of proteins serve as efficient pathways for vibrational energy to flow. In particular, the α helix has been speculated to provide a conduit for vibrational energy transport to and from reaction centers and across cell membranes.[9,14]

In this article, we explore the nature and rate of vibrational energy flow in α helical peptides, a major structural element of proteins, and compare this with energy transfer in coil segments of proteins. We calculate the rate of vibrational energy transfer in the five largest α helices of myoglobin, which range from 16 to 24 residues. We find that the large majority of normal mode vibrations in the helices are localized, so that intramolecular energy flow from one end of the helix to the other is largely due to anharmonic coupling of the normal modes. The same scenario also holds for one-dimensional (1D) glasses,[15] in which only the very lowest frequency normal modes span the glass, while the vast majority of normal modes are localized. In a 1D glass, energy transfer from a localized mode to a low-frequency bath mode is slow and does not influence the energy flow rate from the higher-frequency, localized mode.[16] We shall see that this is the case for energy transfer rates from most helix modes, too. Finally, we examine the role of structure in energy transfer, comparing energy transfer rates from vibrational modes of a helix to energy transfer rates in coils. Variation of the energy transfer rate with frequency and temperature in coils is similar to that in helices, where on average the anharmonic decay rate is faster than in coils by about a factor of 3. Energy transfer in the α helices is not especially efficient and is comparable to transfer along other portions of the protein backbone. Whether or not the polypeptide chain forms a helical structure, vibrational energy transfer within it parallels anharmonic decay of vibrational states in 1D glasses.

Connections between energy landscapes of proteins, clusters, and glasses have been exploited for some time.[17,18] In this paper,

† Part of the special issue "R. Stephen Berry Festschrift".

10.1021/jp0206119 CCC: $22.00
Published on Web 09/13/2002

Figure 1. Ribbon diagram of sperm whale myoglobin. Normal modes and vibrational energy transfer rates in the five largest helices, labeled A, B, E, G, and H, are calculated. These results are compared with the energy transfer rates in the two largest coil segments, CD and EF.

we compare mechanisms for energy transfer in α helices and coil segments of proteins with that in 1D glasses. Our focus is on the fastest relaxation time scale, when the protein or glass relaxes within a local minimum of the potential, and we address anharmonic decay of the normal modes. Recent theoretical and computational work[16,19,20] has helped elucidate the nature of anharmonic decay of normal modes in a glass. The simplest case is a 1D glass, for which all but of order $N^{1/2}$ of the N normal modes of vibration are localized spatially to regions smaller than the glass, increasingly so as the mode frequency increases.[15] Excitations of localized normal modes in a glass, called locons,[20] cannot transport energy from one end of the glass to the other. Locon transport in a glass arises from anharmonic coupling of overlapping localized normal modes in resonance.[16,20] We shall see that most normal modes of the five largest α helices and two largest coil segments of myoglobin are also localized. It was recently pointed out that energy from a localized mode in myoglobin is transferred to a small number of resonant modes that overlap in space,[21] which is the principle for locon transport in a glass.[16,20] One consequence of localization in a 1D glass is the nearly temperature-independent energy transfer rate from modes with frequency $\omega \gg k_B T/\hbar$. We show below that the same holds for higher frequency modes involving backbone vibrations of helices and coils, including the well-studied amide I band.

In the following section we present computational results of vibrational energy transfer rates in the five largest α helices of myoglobin. In section 3, we introduce a model of a 1D glass whose force constant distribution is parametrized to match that of the helices, and comparisons are made between normal mode distributions and energy transfer rates in the model 1D glass and in the α helices of myoglobin. In section 4, we compare results for energy transfer in helices with energy transfer in the two largest coil segments of myoglobin. Concluding remarks are given in section 5.

2. α-Helices

We consider first the normal modes of the five largest α helices of myoglobin, the A, B, E, G, and H α helices, which are indicated in Figure 1. The number of residues in each helix is 16, 16, 20, 19, and 24 for the A, B, E, G, and H helices, respectively. The work reported in this section parallels that summarized in a recent letter,[22] where energy transfer rates in the same helices are reported.[23] Computation of the normal modes was carried out using the program package MOIL, which was written by Elber and co-workers.[24] Coordinates for the atoms in the helices were taken initially from the minimum-energy structure of myoglobin, and the new minimum energy structures for each helix were subsequently computed, followed by the normal modes. The normal mode frequencies for the five helices range from about 3 to 1850 cm^{-1}, as well as a range of higher frequency modes above 3100 cm^{-1} corresponding to CH, NH, and OH stretches that we shall not consider here. The

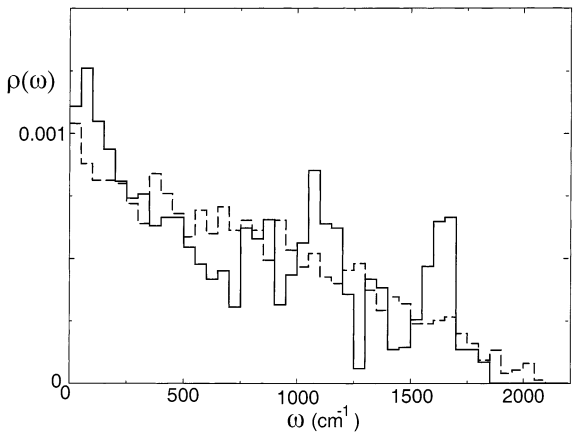

Figure 2. Normalized distribution of normal-mode frequencies, binned into 50 cm^{-1} intervals, of the helices (solid line) and the model 1D glass described in the text (long dashes).

density of normal modes of the helices as a function of mode frequency is plotted in Figure 2. The mode density is highest at low frequency, and it declines with substantial fluctuations as the frequency increases to the band edge around 1850 cm^{-1}. In describing energy flow, it is important to determine the extent to which a normal mode spans the helical peptide. In doing so, we might usefully characterize a polypeptide as a disordered chain of atoms. In a harmonic periodic chain, the normal modes carry energy without resistance from one end of the 1D crystal to the other; however, the vast majority of normal modes of an aperiodic chain are spatially localized and cannot carry heat. We might therefore expect many normal modes of polypeptides to be likewise localized in space.

As a measure of the number of residues contributing to a mode, we calculate the information entropy,

$$S = -\sum_{i=1}^{N_{res}} p_i \ln p_i \qquad (1)$$

where N_{res} is the total number of residues in the helix and p_i is the projection of all coordinates of a residue onto a normal mode of the helix. If vibrations of each residue contribute equally to a normal mode then $S = \ln N_{res}$, whereas $S = 0$ if a normal mode vibration is localized to a single residue. Then e^S is roughly the number of residues that a normal mode spans. The average value of e^S for the 5 helices vs mode frequency is plotted in Figure 3. At frequencies below ≈200 cm^{-1}, the modes span roughly 12 residues, about two-thirds the number of residues (16−24) that make up the helices, where there are on average 19 residues/helix. At higher frequency, there is a gradual decline to participation of 1 to 6 residues, with the larger number involving modes where atoms vibrate along the backbone. For instance, modes that lie in the amide I band, in the range 1600−1700 cm^{-1}, involve larger numbers of residues than modes at somewhat lower or higher frequencies. It is noteworthy that the overall form of $\langle e^S \rangle$ with ω is similar to that of the participation number, ξ, in 1D glasses. The participation number of mode α is defined by $\xi_\alpha = (\Sigma_i (e_n^\alpha)^4)^{-1}$, where e_n^α are the coefficients of normalized vibrational eigenstates and N is the number of atoms in the 1D glass. We found a variation of $\xi \sim \omega^{-2}$ for a model of a 1D glass fits the numerically calculated participation number very well,[16] consistent with theoretical expectations for the localization length.[15] To improve on this, the finite size as well as the large-ω limiting value of 1 can be accounted for by the function $\xi(\omega) \approx \alpha/((3\alpha/2N) + \omega^2) + 1$, where N is the number of atoms in the 1D glass and α is a measure of disorder.

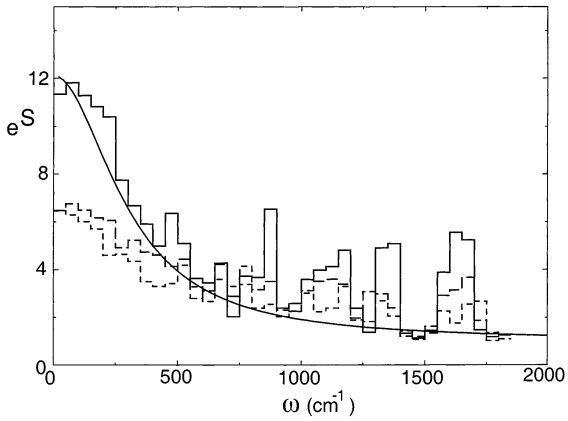

Figure 3. Histograms for e^S plotted as a function of ω. The upper histogram (solid line) is e^S, a measure of the number of residues of the helix that participate in a normal mode vibration, averaged over all modes of the helices in 50 cm^{-1} intervals. The middle, dashed histogram corresponds to e^S for two helices of myoglobin (G and H) truncated to 10 residues. The lowest histogram (short dashes) is the average value of e^S for the CD and EF coil segments, each containing 10 residues. The curve near the upper histogram is the functional form $e^S = \alpha/(\beta + \omega^2) + 1$ discussed in the text, with $\alpha = 1 \times 10^6$ and $\beta = 9 \times 10^4$.

Then when $\omega \rightarrow 0$, we have $\xi \approx 2N/3$, which is the value of the participation number of a periodic chain.[25] Assuming that $\langle e^S \rangle$ varies with ω in a similar way, we compare our numerical results for the helices with an equation of the form $\alpha/(\beta + \omega^2) + 1$. Since there are $N_{res} = 19$ amino acids on average, we take $\alpha/\beta = 2N_{res}/3 - 1 = 12$ to fit the small-ω limit. The result for $\beta = 9 \times 10^4$ is plotted in Figure 3, where we see reasonable agreement with $\langle e^S \rangle$ for the helices, apart from values at several frequencies where normal modes involve backbone vibrations, such as the amide I and II vibrations accounting for the peak from 1550 to 1700 cm^{-1} and the amide III band near 1300 cm^{-1}.

Most normal modes of the helices, like those of an aperiodic chain, cannot carry energy from one end to the other. Anharmonicity generates energy transfer among the localized normal modes. In our calculations of energy transfer we consider only the contribution of cubic anharmonic terms and neglect all terms of higher order, which is reasonable if we restrict ourselves to low temperatures. At low temperatures, the energy transfer rate is dominated by processes that involve the decay of a vibrational excitation into two others, such that $\omega_\alpha = \omega_\beta + \omega_\gamma$. The energy transfer rate, W_α, from mode α is then given by[26]

$$W_\alpha = \frac{\hbar\pi}{8\omega_\alpha} \sum_{\beta,\gamma} \frac{|\Phi_{\alpha\beta\gamma}|^2}{\omega_\beta \omega_\gamma} (1 + n_\beta + n_\gamma)\delta(\omega_\alpha - \omega_\beta - \omega_\gamma) \quad (2)$$

where n_α is the occupation number of mode α, which at temperature T we take to be

$$n_\alpha = (e^{\hbar\omega_\alpha/k_B T} - 1)^{-1} \quad (3)$$

The matrix elements $\Phi_{\alpha\beta\gamma}$ appear as the coefficients of the cubic terms in the expansion of the interatomic potential in normal coordinates, computed numerically as

$$\Phi_{\alpha\beta\gamma} = (\partial^2 V/\partial Q_\alpha \partial Q_\beta|_{Q_0+\delta Q_\gamma} - \partial^2 V/\partial Q_\alpha \partial Q_\beta|_{Q_0-\delta Q_\gamma})/2\delta Q_\gamma \quad (4)$$

where Q_α is a mass-weighted normal coordinate and Q_0 is the equilibrium position of the helix in normal coordinates.

We have computed the vibrational energy transfer rate as a function of mode frequency with eq 2 for the five largest α helices of myoglobin. The results for each individual helix at $T = 45$ K are shown in Figure 4, where we have averaged W_α over all modes in 50 cm^{-1} intervals. We see in Figure 4 that the variation of decay rate with mode frequency for each helix is similar with the exception of a few strikingly high rates, in particular a high rate of about 18 ps^{-1} just above 1500 cm^{-1} in the B helix. The anomalously high rate in the B helix near 1500 cm^{-1} involves energy flow from a vibration of largely the carboxyl group of aspartate at 1544 cm^{-1} to two skeletal aspartate vibrational modes at 738 and 806 cm^{-1}.

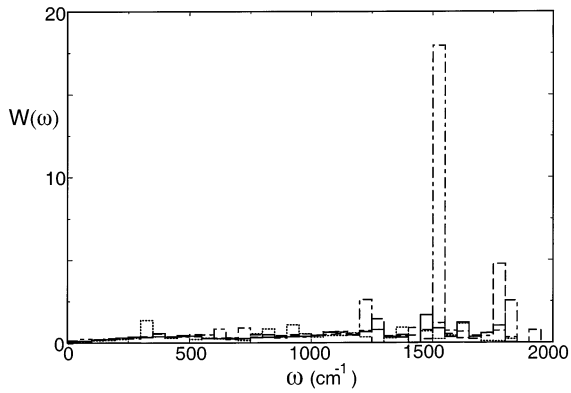

Figure 4. Vibrational energy transfer rates, W, in ps^{-1} for the five largest α helices of myoglobin plotted as a function of mode frequency, ω. The temperature is 45 K. Rates in the A, B, E, G, and H α helices are plotted as dashes, dot−dashes, dots, long dashes, and a solid line, respectively.

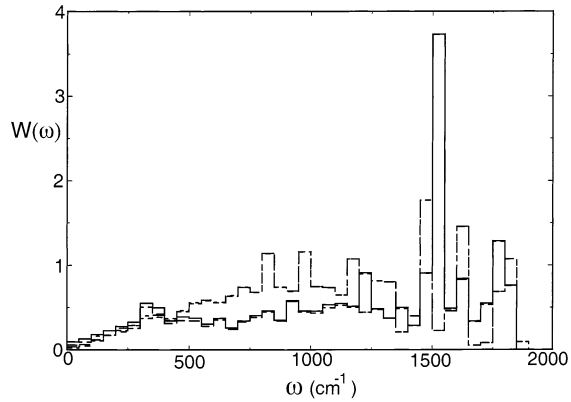

Figure 5. Average vibrational energy transfer rate, W, in ps^{-1} for the five largest α helices of myoglobin plotted as a function of mode frequency, ω, at 15 K (long dashes) and 45 K (solid line). Also plotted is the average vibrational energy transfer rate in the 1D glass model described in the text, where $T = 15$ K (dashes) and 45 K (dot−dashes). Energy transfer rates in the model are higher than in the helices at low frequency but are similar above $\omega \approx 700$ cm^{-1}. Temperature dependence of the rate in both the helices and 1D glass is typically small at higher frequency, above about 400 cm^{-1}.

The average vibrational energy transfer rate in all the helices as a function of frequency is plotted in Figure 5, where the temperatures were chosen to be $T = 15$ and 45 K. Vibrational energy transfer rates are averaged over the vibrational modes of all helices in 50 cm^{-1} intervals. We observe in Figure 5 that the vibrational energy transfer rates are not very sensitive to temperature above about 500 cm^{-1}, with the slight exception of modes with frequencies in the range 1700−1750 cm^{-1}. Temperature dependence of the energy transfer rate implies that energy is flowing directly into low-frequency modes of the helices. Since the temperature dependence largely decreases with increasing mode frequency, we can conclude that as the mode frequency increases there is less direct energy transfer to low-

frequency modes. Such a trend, as we shall see below, is characteristic of energy transfer in a 1D glass. This trend arises because the frequencies of modes that are localized in space tend to "repel" one another;[20,16] modes with similar frequencies do not overlap in space, as will be discussed below. As a consequence, energy transfer to modes with similar frequencies and the remainder to low-frequency modes occurs very slowly. There is as mentioned an exception to this trend at 1700−1750 cm^{-1}, which lies just above the amide I band. We have found that the modes for which the decay rate is temperature dependent correspond to CO stretches in certain side chains, particularly belonging to the glutamine residue of the A, B, and H helices. Significant character of the same CO stretch is found for modes in this frequency range that lie about 15−20 cm^{-1} apart, and a mode of the latter frequency that overlaps the side chain is available for energy transfer. Decay rates of the CO stretches of the amide I band, from about 1600 to 1700 cm^{-1}, are not very temperature sensitive, as has also been observed experimentally.[7] We note that the measured decay rate of the amide I band is about 0.5 ps^{-1},[7,8] somewhat faster than the 0.3 ps^{-1} that we have calculated, though significant differences in the decay rate are found depending on the location within the band; for instance, lifetimes as long as 15 ps are observed at the blue side of the amide I band.[9] The difference between measured and calculated decay rates could arise from the fact that neither residues of loops nor water molecules are included in these calculations, which are carried out only to third order in the anharmonicity; each of these factors would tend to reduce the rate.

We mention that the lifetime of the CO stretch in MbCO is also nearly independent of temperature from 10 to 300 K.[10,11] A weak temperature dependence of the lifetime might not be quite as unexpected as for amide I band vibrations, since the CO stretch frequency of roughly 1950 cm^{-1} lies some 100 cm^{-1} above the band of protein vibrations. Low-order anharmonic coupling cannot couple the CO to the lowest-frequency, delocalized modes. Weak coupling to low-frequency modes would also be enhanced by the likelihood that the frequencies of localized normal modes overlapping in space are widely spaced. The photon echo experiments of Fayer, Dlott, and coworkers provide the pure dephasing rate over the same range of temperatures. The rate of pure dephasing, of course, does not depend on resonant coupling between vibrational modes, so that coupling to low-frequency modes, which provides the strongest temperature dependence of the rate, is not restricted by resonance requirements. Indeed, for temperatures below the glass transition temperature of the protein, the pure dephasing rate appears to follow a power-law dependence on temperature, with a power of about 1.3.[10,11] Recent calculations of the pure dephasing rate of a ligand vibration coupled by dipole−dipole interactions to an α-helix also reveal an apparent power-law dependence of the pure dephasing rate with a power between 1 and 2.[27]

3. 1D Glass

We turn now to a comparison of anharmonic decay rates of vibrational states in helices with decay in an anharmonic 1D glass. Such a comparison can provide insight into the variation of the energy transfer rate with mode frequency and with temperature, as we discuss in this section. Here we modify a model presented previously[22] in a way that improves agreement between the normal mode density of the model and that of the helical peptide.

Our model for an anharmonic 1D glass is a chain of N equally spaced atoms of unit mass connected by random forces. For the calculations discussed below we take an ensemble of five chains of $N = 500$ atoms. This gives us as many chains in the ensemble as we have helices, and the number of vibrational modes/chain matches the average of 499 vibrational modes/helix (where we are excluding helix modes with frequencies above 3000 cm^{-1}). The potential energy of the glass is given by $V = V_2 + V_3$, where V_2 is the potential energy to second order,

$$V_2 = \frac{1}{2}\sum_{n=1}^{N} f_n (u_n - u_{n+1})^2 \tag{5}$$

with u_n the displacement of atom n from equilibrium and f_n the force constant. (Since we express frequencies in cm^{-1}, it will be convenient to express f_n in units of $(cm^{-1})^2$.) Anharmonicity arises from

$$V_3 = \frac{1}{6}\sum_{n=1}^{N} g_n (u_n - u_{n+1})^3 \tag{6}$$

The normal mode frequencies are obtained from the eigenvalues of the Hessian matrix, whose diagonal elements are $d_n = f_{n-1} + f_n$. By contrast, the diagonal elements, d, of the Hessian matrix for the α helices are the sums of numerous terms accounting for a larger number of local interactions. In fact, the distribution of the latter, shown in Figure 6, resembles the positive half of a Gaussian centered at 0, whose standard deviation we have found to be 9.5×10^5 $(cm^{-1})^2$. We take the force constants, f_n, to be randomly distributed in an exponential distribution such that the standard deviation of the distribution of $d_n = f_{n-1} + f_n$, the diagonal elements of the Hessian of the model, matches that for the helices. The distribution of d_n appears to be similar to that of the diagonal matrix elements of the Hessian for the helices, as seen in Figure 6. We have also introduced a large-f_n cutoff of 1.7×10^6 $(cm^{-1})^2$ to prevent mode frequencies much higher than the band edge for the helices. Then f_n is taken randomly from an exponential distribution with standard deviation 4.0×10^5 $(cm^{-1})^2$ and cutoff 1.7×10^6 $(cm^{-1})^2$. For the diagonal elements of the Hessian matrix of this model we find a standard deviation of 9.0×10^5 $(cm^{-1})^2$, close to that for the helices. In Figure 2 we compare the normal mode density of the harmonic 1D glass consisting of 5 chains of $N = 500$ with the normal mode density of the helices. The secular variation of the mode density of the helices with mode frequency reveals specific features reflecting their constituents and interactions. Nevertheless, these features appear as fluctuations around the mode density of the model.

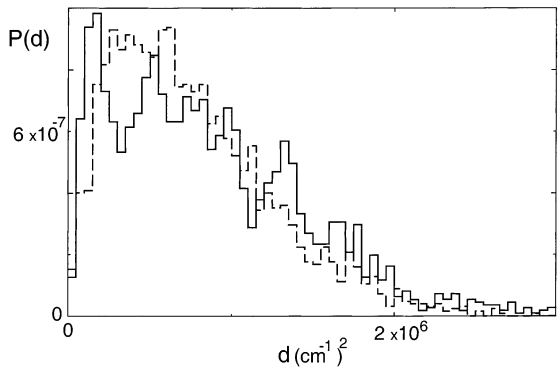

Figure 6. Normalized distribution of diagonal matrix elements of the Hessian matrix, in $(cm^{-1})^2$, for the five largest α helices of myoglobin (solid line) and for the model 1D glass described in the text.

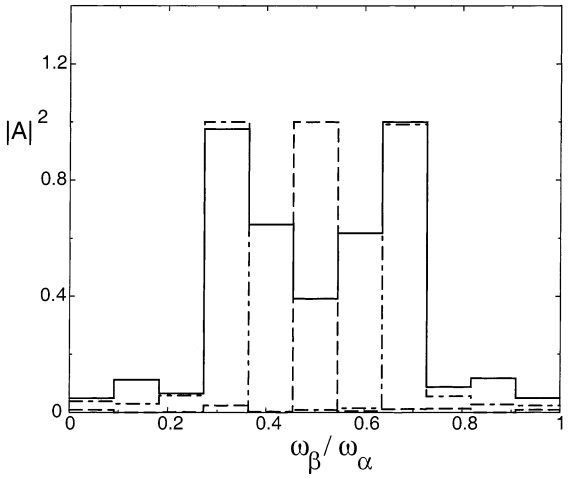

Figure 7. Average value of $|A|^2$, defined by eq 8, for coupling a glass or helix mode with frequency ω_α to two others with frequencies ω_β and ω_γ ($=\omega_\alpha - \omega_\beta$), as a function of $\omega_\beta/\omega_\alpha$. Units of $|A|^2$ are arbitrary. The solid line corresponds to the $N = 500$ 1D glass model at $\omega_\alpha \approx 1500$ cm^{-1}. The long-dashed histogram corresponds to average $|A|^2$ for the five helices at $\omega_\alpha \approx 1500$ cm^{-1}. The dot−dashed histogram corresponds to helices at $\omega_\alpha \approx 1200$ cm^{-1}. We observe that the largest values of $|A|^2$ couple modes with frequencies ω_β and ω_γ ($=\omega_\alpha - \omega_\beta$) between about $\omega_\alpha/3$ and $2\omega_\alpha/3$ to modes with frequencies of ω_α. Peaks around $\omega_\beta/\omega_\alpha = 0.5$ include contributions from 2:1 Fermi resonances.

Vibrational energy transfer in the model glass arises from the anharmonicity, V_3, given by eq 6. The cubic anharmonic constants should vary as $g = cf/a$, where a is a lattice spacing and c is a constant of order 1. The constant c/a is our one fitting parameter, chosen so that the average decay rates in the glass match those in the helices; a is a few Å so that c/a should lie in the range 0.1−1 Å^{-1}. If f is the average value of the force constant, then we set all $g_n = (c/a)f_n$. The energy transfer rate, W_α, is given by eq 2, where for this model it is straightforward to calculate

$$\Phi_{\alpha\beta\gamma} = \sum_{n,n',n''}^{N} \frac{\partial^3 V}{\partial u_n \partial u_{n'} \partial u_{n''}} e_n{}^{\alpha} e_{n'}{}^{\beta} e_{n''}{}^{\gamma} Q_\alpha Q_\beta Q_\gamma \qquad (7)$$

where the sum is over all sites n, n', and n''. In Figure 5 we compare the vibrational energy transfer rate in the glass to the energy transfer rate in the helices at $T = 15$ and 45 K. For the cubic anharmonic coefficients of the glass we have chosen $c/a = 1$ Å^{-1}, which yields energy transfer rates that agree reasonably well with the transfer rates of the helices. We find that the transfer rate becomes less dependent on temperature with increasing mode frequency, the same trend as for the helices. As mentioned earlier, the small temperature dependence of the energy transfer rate from higher-frequency modes implies that little energy decays to the low-frequency modes of the glass.

Since energy flow to the large density of low-frequency modes is slow, there must be relatively weak coupling between high-frequency localized modes and low-frequency modes. We illustrate this in Figure 7, where we plot the matrix elements in eq 2 that couple mode α to a pair of modes β and γ or to a second mode β with frequency $\omega_\beta \approx \omega_\alpha/2$. Calling these matrix elements

$$|A|^2 \equiv \frac{\hbar\pi}{8} \frac{|\Phi_{\alpha\beta\gamma}|^2}{\omega_\alpha \omega_\beta \omega_\gamma} (1 + n_\beta + n_\gamma) \qquad (8)$$

we plotted the relative values of $|A|^2$, coupling mode α with frequency ω_α to mode β with frequency ω_β and mode γ with frequency $\omega_\gamma = \omega_\alpha - \omega_\beta$, averaged over modes of the ensemble of five chains in intervals of ≈150 cm^{-1}. Values of ω_β must be $0 < \omega_\beta < \omega_\alpha$, and we plot $|A|^2$ as a function of $\omega_\beta/\omega_\alpha$, which falls in the range 0−1. Since $\omega_\alpha = \omega_\beta + \omega_\gamma$, large values of $|A|^2$ near 0 or 1 would indicate strong coupling to low-frequency modes. We plot $|A|^2$ as a function of $\omega_\beta/\omega_\alpha$ for the 1D glass at $\omega_\alpha \approx 1500$ cm^{-1}. To compare with the helices, we have also calculated the average $|A|^2$ for the helices at $\omega_\alpha \approx 1500$ cm^{-1}, as well as at $\omega_\alpha \approx 1200$ cm^{-1}. We see that in each case strongest coupling is between a mode with frequency ω_α and pairs of modes in resonance with mode α whose frequencies lie largely in the range $\omega_\alpha/3$ to $2\omega_\alpha/3$. For the 1D glass and the helices at $\omega_\alpha \approx 1500$ cm^{-1}, largest coupling is to modes where $\omega_\beta \approx \omega_\alpha/3$ and $\omega_\beta \approx 2\omega_\alpha/3$. Large coupling at $\omega_\alpha/2$ seen for the helices at $\omega \approx 1200$ cm^{-1} arises predominantly from contributions of 2:1 Fermi resonances.

The observed distribution of coupling matrix elements is due to the fact that frequencies of normal modes that are localized to the same regions of space tend to be spread apart. The frequencies of nearby localized oscillators thus appear to repel one another. Consider, for instance, just two oscillators vibrating with frequencies ω_1 and ω_2. If the oscillators are near one another in space, they are coupled to each other by perhaps several hundred cm^{-1}, whereas if they are far from each other the coupling between them is small. For the vibrational energy to remain localized in one oscillator, the difference in their frequencies, $|\omega_1 - \omega_2|$, must be several hundred cm^{-1} if the oscillators are close in space, whereas there is no such restriction if they lie far apart. Such "mode repulsion" of nearby localized oscillators has consequences on the cubic anharmonic terms that couple them. Cubic anharmonic coupling of at least one high-frequency, localized mode to other modes is large only when the modes overlap in space. In this case, the normal modes that are coupled are widely spread in frequency; cubic terms coupling localized modes of similar frequency are therefore often relatively small. The latter are the terms that also couple a given mode with excess energy to the low-frequency bath modes, since the remainder of the energy not transferred to a mode of similar frequency must end up there. Thus direct energy transfer from a localized mode of the 1D glass to another localized mode of similar frequency and to a low-frequency bath mode is relatively slow, owing to the small size of the cubic coupling term that enables this process.

The influence of spatial location of two normal modes on the frequency difference of these vibrational modes is shown in Figure 8. We locate the largest component of each vibrational mode, α, and calculate the probability, $P(\Delta\omega)$, that, for another mode, β, whose largest component lies a certain distance away from the largest component of mode α, the difference in frequency between the two modes is $\Delta\omega = |\omega_\alpha - \omega_\beta|$. We consider only localized modes, α, whose frequency, ω_α, falls between 1000 and 2000 cm^{-1}. Probabilities are calculated for $\Delta\omega$ in intervals of 20 cm^{-1} up to $\Delta\omega = 600$ cm^{-1}. Results for the one-dimensional glass are shown in Figure 8a, and results for the G and H helices of myoglobin are shown in Figure 8b. The dashed histograms in both parts a and b of Figure 8 are averages over all pairs of vibrational eigenstates, regardless of the distance between the largest components of α and β. Consider first the 1D glass shown in Figure 8a. For any pair of modes α and β, there is just as much chance that the difference of their vibrational frequency is small, e.g., less than 100 cm^{-1}, as it is fairly large, 500−600 cm^{-1}. The solid-line histogram gives the probability of finding $\Delta\omega$ when the maximum component of the eigenstates α and β are on nearest-neighbor

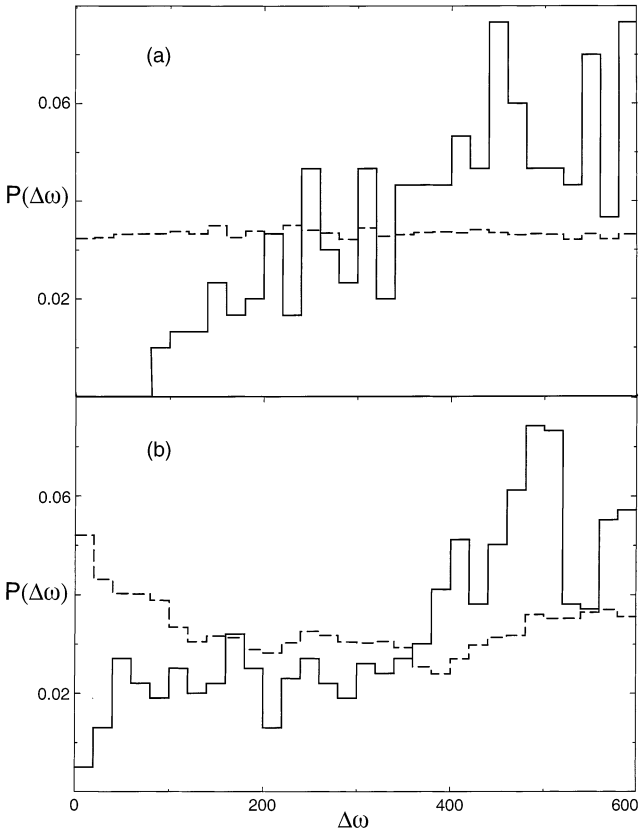

Figure 8. Probability, $P(\Delta\omega)$, of finding a pair of vibrational modes with frequency difference $\Delta\omega$ in (a) the 1D glass model and (b) the G and H α-helices of myoglobin, when at least one of the modes is localized with frequency ω in the range 1000 $cm^{-1} < \omega < 2000$ cm^{-1}. Dashed lines are probabilities for any pair of modes with frequency difference $\Delta\omega$, regardless of their distance from one another in space. The solid lines are results only for vibrational modes that lie near one another in space. In (a), they correspond to vibrational eigenstates whose maximum component lies over nearest-neighbor atoms in the 1D glass. In (b), the pairs of modes are restricted to those whose largest components lie within 2 Å in the helix.

atoms of the glass. In this case, we find no pairs of modes with $\Delta\omega \approx 80$ cm^{-1} and about half as many as found on average for any distance when $\Delta\omega$ is between about 100 and 200 cm^{-1}. Instead, larger values of $\Delta\omega$, closer to 500 or 600 cm^{-1}, are expected to be found when the vibrational eigenstates α and β are localized to neighboring atoms. We thus see for the 1D glass that vibrational modes localized close to one another in space tend to have frequencies that are quite different. Turning to Figure 8b, we observe the same pattern for the G and H α-helices of myoglobin. The dashed line again gives the probability of finding modes whose frequency difference is $\Delta\omega$ for all pairs of modes, regardless of the distance between their largest components, with one member of the pair a localized mode such that 1000 $cm^{-1} < \omega < 2000$ cm^{-1}. In this case, when we ignore the distance of the modes from one another, there is generally a somewhat larger chance of finding pairs of modes whose frequency difference is small, below about 100 cm^{-1}. However, if we only consider pairs of modes whose largest components overlap atoms that lie less than 2 Å from each other, we obtain the solid-line histogram in Figure 8b. As for the 1D glass, we see that if pairs of localized modes lie nearby in space, there is a propensity for their frequency differences to be large, in this case around 500 cm^{-1}, rather than small, e.g., below 200 cm^{-1}. Such a propensity diminishes as we consider localized normal modes whose largest components lie farther away from each other. For distances between

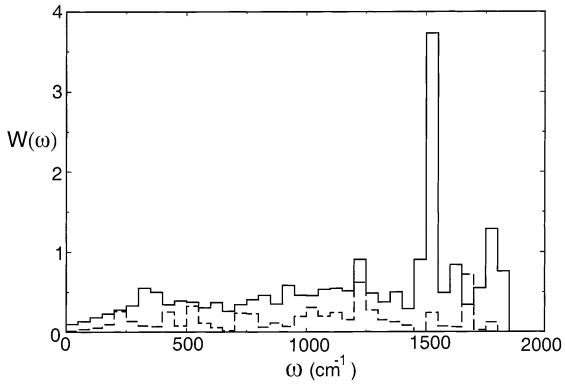

Figure 9. Average vibrational energy transfer rates, W, in ps^{-1} for the five largest α helices of myoglobin (solid line) and the two largest coil segments (long dashes) plotted as a function of mode frequency, ω, at 45 K.

4 and 5 Å, as well as larger distances, we find $P(\Delta\omega)$ to be essentially the same as the dashed histogram, for which the distance between the modes is ignored. Because of the apparent repulsion of frequencies of strongly localized modes, matrix elements coupling two high-frequency modes close in frequency and a low-frequency mode are generally small, as we saw in Figure 7. Although shown here for only helices of myoglobin, we observe a similar separation of mode frequencies for spatially nearby localized modes of the complete protein.[28] Given the close connection between the vibrations of proteins and 1D glasses, we expect the temperature dependence of the anharmonic decay rate of higher-frequency localized modes to be often small in proteins.

4. Coils

We now compare vibrational energy transfer rates in α helices presented in section 2 with energy transfer rates in coils. We have calculated vibrational energy transfer rates in the two largest coil segments of myoglobin, the CD and EF segments, indicated in Figure 1. Each of these segments contains 10 residues. As for the α-helices, we computed the information entropy, S, where e^S is a measure of the number of amino acids that participate in a normal mode vibration. The result is plotted alongside the helix results in Figure 3, where we plot the average value of e^S as a function of frequency in 50 cm^{-1} intervals. Just as for the helices, the normal modes of the coils are fairly delocalized over the polypeptide at low frequency but become increasingly localized above about 200 cm^{-1}. Because the length of the peptide influences the value of e^S at low frequency, we compare e^S for the coil segments with e^S for two helices that also contain 10 residues, where we use the first 10 residues of the G and H α-helices of myoglobin. We observe in Figure 3 that the normal modes of the helices are generally somewhat more delocalized than those of the coil segments, extending over about one more residue of the polypeptide, likely due to the hydrogen-bonded network that is absent in the coils.

Vibrational energy transfer rates in the coil segments are plotted in Figure 9 together with results for the helices, where we have chosen $T = 45$ K. We found little difference in the energy transfer rates between the 10-residue helices and the complete ones, so we simply compare energy transfer rates in the coils with the average energy transfer rates in the complete helices. The average energy transfer rate in the α helices over the complete band of vibrational mode frequencies, 0.54 ps^{-1}, is about a factor of 3 greater than the average energy transfer rate in the coils, which is 0.16 ps^{-1}, where again the difference

is due to the hydrogen-bonded network of the helices. Variation of the energy transfer rate with mode frequency is similar in both helices and coils, resembling the variation seen for 1D glasses in the previous section. The temperature dependence of the energy transfer rate is noticeable only at low frequency (not shown in figure), paralleling closely the variation in the α-helices and again consistent with the small temperature variation of the energy transfer rate measured for the amide I band of myoglobin from about 10 to 300 K.[7]

5. Concluding Remarks

We have calculated rates of vibrational energy transfer in the five largest α helices and two largest coil segments of myoglobin and compared them to each other and to rates of vibrational energy transfer in 1D glasses. The majority of normal modes of the helices and coils, essentially all those with frequencies larger than about 200 cm^{-1}, involve vibrations of only a subset of all the residues of the peptide. Variation of the number of residues participating in a normal mode vibration with mode frequency follows a functional form similar to that for the participation of the number of atoms in a normal mode vibration with mode frequency in a 1D glass. Because most normal modes of a polypeptide, like those of a 1D glass, are localized, they cannot transfer heat from one end of the polypeptide to the other. Energy transfer among normal modes and throughout the molecule is enabled by anharmonic coupling. Though in principle any mode of the helix or coil is directly coupled anharmonically to a large number of low-frequency bath modes of the polypeptide, the coupling is usually small, and direct energy transfer to low-frequency modes is often slow. For this reason, there is little temperature dependence of energy transfer from higher-frequency modes of either coils or helices. These results imply that energy transport in α helices of proteins is not particularly efficient, in contrast to speculation that they may serve as efficient conduits for vibrational energy transfer.[14,9] We see in Figure 9 that the energy transfer rate in a helix is about a factor of 3 faster than in a coil. Both resemble energy transfer in 1D glasses, which are not especially good conductors. Earlier MD simulations[29] on cytochrome *c* also revealed no particular preference for energy propagation through well-defined secondary structures. In a recent letter,[22] we estimated that the coefficient for energy diffusion in α helices would be very roughly 10 $Å^2$ ps^{-1}, and we expect this to be similar in coil segments as well. Recent interesting molecular dynamics simulations[30] reveal that fast energy transfer from heme to water in CO−myoglobin is due to funneling of energy through isopropionate groups of the heme directly to water and so does not involve energy flow through the globin. In this way, energy is transferred out of the heme to water in a few picoseconds rather than the greater than 20 ps required if energy flowed from the heme to the globin and then to water.[31]

Energy transfer from most vibrational modes in polypeptides, as in 1D glasses, occurs predominantly by hopping of localized vibrations along the chain resulting from anharmonic coupling of spatially overlapping localized modes in resonance. As discussed and illustrated for both glasses and helical peptides, the frequencies of normal modes localized to nearby regions of these systems generally lie far apart. This means that anharmonic coupling between two high-frequency modes and a low-frequency mode is often weak, yielding a typically small temperature dependence of the decay rate at higher frequency, consistent with the observed[7] weak temperature dependence of the amide I band, as well as the weak temperature dependence of the CO stretch lifetime in CO−myoglobin.[10] We find the vibrational energy transfer rate to be of order 1 ps^{-1} for a wide range of mode frequencies and temperatures, similar to energy transfer rates in small molecules, despite the high density of low-frequency bath modes.

Acknowledgment. It is a pleasure to dedicate this paper to Steve Berry. This work was supported by the National Science Foundation (NSF Grant CHE-0112631), by a New Faculty Award from the Camille and Henry Dreyfus Foundation, and by a Research Innovation Award from the Research Corporation.

References and Notes

(1) Gruebele, M. *Adv. Chem. Phys.* **2000**, *114*, 193.

(2) Keske, J. C.; Pate, B. H. *Annu. Rev. Phys. Chem.* **2000**, *51*, 323.

(3) Leitner, D. M.; Wolynes, P. G. *Chem. Phys. Lett.* **1997**, *280*, 411.

(4) Leitner, D. M. *Int. J. Quantum Chem.* **1999**, *75*, 523.

(5) Chandler, D.; Kuharski, R. A. *Faraday Discuss. Chem. Soc.* **1988**, *85*, 329 and references therein.

(6) Nordholm, S. *Chem. Phys.* **1989**, *137*, 109.

(7) Peterson, K. A.; Rella, C. W.; Engholm, J. R.; Schwettman, H. A. *J. Phys. Chem B* **1999**, *103*, 557.

(8) Hamm, P.; Lim, M.; Hochstrasser, R. M. *J. Phys. Chem. B* **1998**, *102*, 6123.

(9) Xie, A.; van der Meer, L.; Hoff, W.; Austin, R. H. *Phys. Rev. Lett.* **2000**, *84*, 5435.

(10) Rella, C. W.; Rector, K. D.; Kwok, A.; Hill, J. R.; Schwettman, H. A.; Dlott D. D.; Fayer, M. D. *J. Phys. Chem.* **1996**, *100*, 15620. Rella, C. W.; Kwok, A.; Rector, K.; Hill, J. R.; Schwettman, H. A.; Dlott, D. D.; Fayer, M. D. *Phys. Rev. Lett.* **1996**, *77*, 1648.

(11) Fayer, M. D. *Annu. Rev. Phys. Chem.* **2001**, *52*, 315.

(12) Seno, Y.; Gō, N. *J. Mol. Biol.* **1990**, *216*, 111. McCammon, J. A.; Harvey, S. C. *Dynamics of proteins and nucleic acids*; Cambridge University Press, New York, 1987. Brooks, C. L.; Karplus, M.; Pettitt, B. M. *Adv. Chem. Phys.* **1988**, *71*, 1.

(13) Roitberg, A.; Gerber, R. B.; Elber, R.; Ratner, M. A. *Science* **1995**, *268*, 1319. Roitberg, A.; Gerber, R. B.; Ratner, M. A. *J. Phys. Chem. B* **1997**, *101*, 1700.

(14) Davydov, A. S. *Solitons in Molecular Systems*; Kluwer Academic: Dordrecht, The Netherlands, 1991.

(15) Matsuda, H.; Ishii, K. *Suppl. Prog. Theor. Phys.* **1970**, *45*, 56.

(16) Leitner, D. M. *Phys. Rev. B* **2001**, *64*, 094201.

(17) Frauenfelder, H.; Sligar, S. G.; Wolynes, P. G. *Science* **1991**, *254*, 1598. Wolynes, P. G.; Onuchic, J. N.; Thirumalai, D. *Science* **1995**, *267*, 1619.

(18) Ball, K. D.; Berry, R. S.; Kunz, R. E.; Li, F. Y.; Proykova, A.; Wales, D. J. *Science* **1996**, *271*, 963.

(19) Taraskin, S. N.; Elliott, S. R. *Phys. Rev. B* **2000**, *61*, 12017, 12031.

(20) Fabian, J.; Allen, P. B. *Phys. Rev. Lett.* **1997**, *79*, 1885. Fabian, J. *Phys. Rev. B* **1997**, *55*, R3328.

(21) Moritsugu, K.; Miyashita, O.; Kidera, A. *Phys. Rev. Lett.* **2000**, *85*, 3970.

(22) Leitner, D. M. *Phys. Rev. Lett.* **2001**, *87*, 188102.

(23) The number of residues in each helix used in ref 22 is slightly different than the number used here. The B, G, and H helices each had two fewer residues than used in this study. In Figure 3 of ref 22, rates plotted below 100 cm^{-1} are erroneously large; this has been corrected in Figure 5 of this paper.

(24) Elber, R.; et al. *Comput. Phys. Commun.* **1995**, *91*, 159. The version used for this study was obtained from http://www.tc.cornell.edu/reports/NIH/resource/CompBiologyTools/moil/.

(25) Allen, P. B.; Kelner, J. *Am. J. Phys.* **1998**, *66*, 497.

(26) Maradudin, A. A.; Fein, A. E. *Phys. Rev.* **1962**, *128*, 2589.

(27) Leitner, D. M. *Chem. Phys. Lett.*, **2002**, *359*, 434.

(28) Yu, X.; Leitner, D. M. To be published.

(29) Wang, Q.; Wong, C. F.; Rabitz, H. *Biophys. J.* **1998**, *75*, 60.

(30) Sagnella, D. E.; Straub, J. E.; Thirumalai, D. *J. Chem. Phys.* 2000, *113*, 7702. Sagnella, D. E.; Straub, J. E. *J. Phys. Chem. B* **2001**, *105*, 7057.

(31) Lian, T. Q.; Locke, B.; Kholodenko, Y.; Hochstrasser, R. M. *J. Phys. Chem.* **1994**, *98*, 11648.